Design of a CMOS Compatible, Athermal, Optical Waveguide

by

Luis Enrique Fernandez

Submitted to the Department of Materials Science and Engineering
in partial fulfillment of the requirements for the degree of

Bachelor of Science in Materials Science and Engineering

at the

MASSACHUSETTS INSTITUTE OF TECHNOLOGY

June 2007

Author .....
Department of Materials Science and Engineering
May 21, 2007

Certified by .....
Lionel C. Kimerling
Thomas Lord Professor of Materials Science and Engineering
Thesis Supervisor

Accepted by .....
Caroline A. Ross
Chairman, Undergraduate Thesis Committee

Design of a CMOS Compatible, Athermal, Optical Waveguide

by

Luis Enrique Fernandez

Submitted to the Department of Materials Science and Engineering
on May 21, 2007, in partial fulfillment of the
requirements for the degree of
Bachelor of Science in Materials Science and Engineering

Abstract

This paper explores a possible design for a CMOS compatible, athermal, optical waveguide. The design explored is a slot waveguide with light guided in the low index material. A design paradigm is proposed which shows the relationship between cross-sectional parameters and their impact on both the effective index of refraction and the thermo-optic coefficient of the device. Two materials choices were explored to serve as the low index material, poly(ether imide) (PI) and poly(methyl methacrylate) (PMMA). The slot waveguide with PI as the low index material had a simulated, device thermo-optic coefficient of -8.5 x $10^{-4}K^{-1}$, and the slot waveguide with PMMA as the low index material had a simulated, device thermo-optic coefficient of 1.7 x $10^{-5}K^{-1}$.

Thesis Supervisor: Lionel C. Kimerling
Title: Thomas Lord Professor of Materials Science and Engineering

Acknowledgments

Thanks to Professor Lionel Kimerling and the entire EMAT Group for their support and guidance throughout the research process, especially to Rong Sun my graduate student advisor for his patience in offering me all the help I needed to produce this thesis.

Thanks to the staff of the Microsystems Technology Laboratories for supporting all of our research endeavors in the field of microphotonics.

Thanks to Tim McClure and Elisabeth Shaw of the Center for Materials Science and Engineering for their assistance in carrying out necessary aspects of this research.

A special thank you to the faculty of the Department of Materials Science and Engineering for their excellent teaching and mentorship.

Thank you, Donna Friedman, for all of your advice and support in helping me to reach this moment in my academic career, I could not have reached this moment without your care and compassion.

Thanks to the Massachusetts Institute of Technology and all of those friends I have had the special privilege of meeting while attending this magnificent academic institution.

Finally, thanks to my family, and in a special way, my mother who has been with me from the start.

Contents

List of Figures

List of Tables

Chapter 1

Introduction

Optical waveguides have been employed in high speed data transfer for a number of years beginning in the 1970's with optical fibers used in telephony. Optical transmission technology has evolved through the decades, and today, virtually all long distance data transfers involve the use of optical fibers and associated devices [8]. The most important improvements in optical technology have come in the form of low loss fibers and wavelength division multiplexing; these improvements allow for the possibility of data transmission speeds in excess of 10 Gb/s [4]. The tremendous demand for high speed communications, which can only be provided by optics, has pulled optical networks closer and closer to the end user. On-chip integrated optics is the new objective; unfortunately significant obstacles to the development of an electronic-photonic integrated chip (EPIC) remain.

The hope of photonics professionals is that an EPIC will provide personal computing many of the same advantages that optical fibers have provided to long distance communication. However, on-chip optics are quite different from fiber optics; two of the most important differences are geometry and mechanism for light confinement. The planar geometries of on-chip waveguides combined with their smaller length scale, allows light to be guided by the excitation of discrete modes rather than by total internal reflection as in fibers.

The operating environment also imposes its own restrictions on the successful development of integrated optics. A high premium on wafer space forces waveguides

with sub-micron dimensions and high density line spacing. The ubiquity of the CMOS processing standard places additional restrictions on the materials available for design due to the adverse economic impact of designing outside of the CMOS standard. High temperatures and temperature fluctuations within IC's result in the need for the development of athermal waveguides, whose performance does not change with temperature. The result of all these restrictions is a fairly limited design space for the development of an EPIC.

This paper focuses on the present state of development of an athermal, CMOS compatible, optical waveguide and proposes a preliminary design based on the results of simulations conducted with Apollo Photonic Solutions Suite (APSS).

Chapter 2

Background

2.1 Slab Waveguide

Light confinement in optical planar waveguides is achieved by a different mechanism than in optical fibers, in which the mode of confinement is total internal reflection in the core of the fiber. Planar waveguides have subwavelength widths rendering conventional linear optical physics models insufficient for a complete understanding of light behavior in such waveguides. Instead, such planar waveguides guide only certain restricted modes of light which are allowed based on the geometry and index contrast of the waveguide. The guided modes result from a solution to the wave equation for the appropriate boundary conditions specific to the geometry of the waveguide. The guided modes are simply the result of the interference pattern generated within the waveguide as different components of waves cross each other traversing in opposite directions.

In a slab waveguide, for example, two plane waves travel down the waveguide zig-zagging from one interface to the other, continuously crossing each other. Where the two waves interfere constructively with each other, the intensity of the wave is at a maximum, and where the two waves interfere destructively, the intensity of the wave is at a minimum. This pattern of maxima and minima is a stable interference pattern because the waves are coming from the same source [6].

For a planar slab waveguide with fixed x thickness and infinite in the yz-plane,

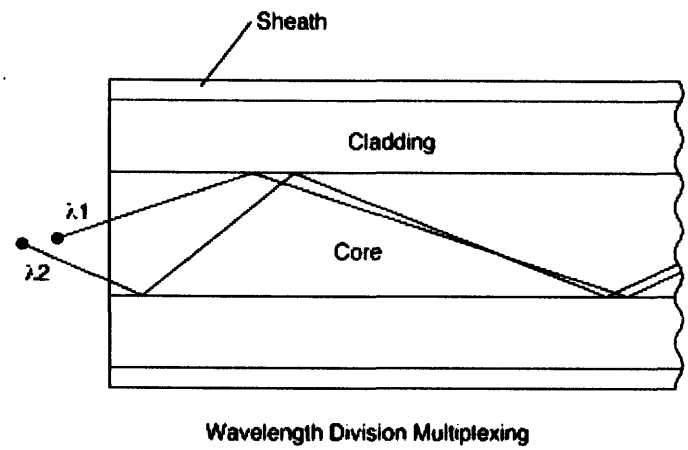

Figure 2-1: Total internal reflection in an optical fiber [4]

the wave equation for the electric field component of light takes the following form:

$$\nabla^2 E_y + k_0^2 n_i^2 E_y = 0$$

where n_i is the index of refraction of the material depending on the location within the waveguide; n_f usually denotes the index of the slab material, n_s the substrate material below the slab, and n_c the cladding material above the slab. The index of the core is greater than both the substrate and cladding indices. And, the wavevector, k_0, is associated with a particular wavelength of light.

The general solution to the wave equation becomes:

$$E_y(x) = E_0 e^{\pm\sqrt{\beta^2 - k_0^2 n_i^2 x}}$$

When β is greater than the product $k_0 n_s$ a guided mode results in the slab. Here, β is simply the z-component of the product $k_0 n_f$. Using the boundary conditions for the slab waveguide, the eigenvalues of β or the discrete guided modes, can be found. The number of guided modes depends on the thickness of the guide as follows:

$$V = k_0 d \sqrt{n_f^2 - n_s^2}$$

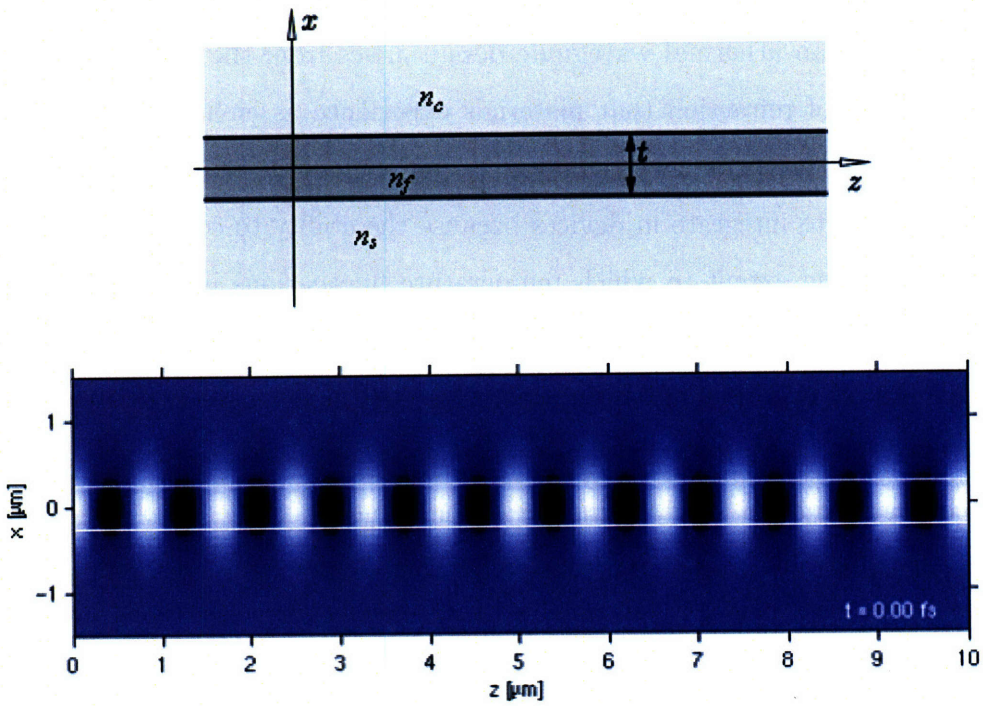

Figure 2-2: Slab waveguide and excited modes in a waveguide[3]

For every $\pi/2$ decrease in V, the normalized thickness of the guide, the number of guided modes decreases by 1. In the equation above, d represents the thickness of the slab guide [6], [5].

2.2 Principles of Athermal Operation

From the analysis of the slab waveguide above, it is apparent that the number and character of the guided modes depends on both the thickness of the waveguide and the index of refraction of the different component materials. The analysis for the slab guide can be extended to all geometries of waveguides by an analogous approach; the main difference will occur in the choices for the relevant boundary conditions. The specific adjustments of the above equations to different waveguide geometries such as channel waveguides and ridge waveguides is beyond the scope of this paper. However, it should be noted that the above analysis concerning the impact of the index of refraction and the dimensions of various parts of the cross-section on the

guided modes in the waveguide is at least conceptually valid.

The need for an athermal waveguide design arises from the need to control the change in index of refraction that materials experience as environmental temperatures fluctuate. A waveguide who's materials' parameters fluctuate with temperature becomes difficult to integrate in devices because the ability to control guided modes will depend on the extent to which temperature fluctuations in the device can be controlled. Precise temperature control requires additional components, and space is at a premium on IC's making this approach to optical integration impractical. An athermal waveguide, on the other hand, relies on materials engineering and intrinsic device characteristics to limit the impact of temperature on the index of refraction.

The normal temperature dependence of waveguide devices is as follows:

$$\frac{1}{L}\frac{dS}{dT} = n_{eq}\alpha_s + \frac{dn_{eq}}{dT}$$

where the left side of the equation represents the dependance of the optical path on temperature. From the above expression, the athermal condition is therefore:

$$\alpha_s + \frac{1}{n_{eq}}\frac{dn_{eq}}{dT} = 0$$

where n_eq is the effective index of refraction of the waveguide device and α_s is the thermal expansion coefficient of the substrate. For an assymetrical slab waveguide whose top cladding is different from the substrate material, the athermal condition has the following form:

$$\frac{1}{L}\frac{dS}{dT} = 0 = \alpha_s + \frac{1}{2n_{eq}^2}\left[\begin{array}{l} \left(n_f^2 - n_c^2\right) V\alpha_f \frac{db}{dV} \\ + \left\{2b + \left(V + \frac{p}{(1+p)\sqrt{b+p}}\right)\frac{db}{dV}\right\} n_f \frac{dn_f}{dT} \\ + \left\{\frac{1}{(1+p)\sqrt{b+p}}\frac{db}{dV}\right\} n_s \frac{dn_s}{dT} \\ + \left\{2\left(1-b\right) - \left(V + \frac{1}{\sqrt{b+p}}\right)\frac{db}{dV}\right\} n_c \frac{dn_c}{dT} \end{array}\right]$$

In the above expression, the constants b and p represent index contrasts between core, cladding, and substrate, and V represents the normalized slab thickness as

discussed in the previous section. The important idea to extract from the above expression is that by combining materials with complementary dn_i/dT and with the appropriate geometry, a waveguide with $dn_{eq}/dT \approx 0$ can be achieved. For example, by pairing a core material with $dn_f/dT \rangle 0$, a substrate material with $dn_s/dT \rangle 0$, and a cladding material with $dn_c/dT \langle 0$, the total effective thermo-optic coefficient, dn_{eq}/dT, might be small enough so that changes in temperature would only slightly affect the guided modes in the waveguide [10].

The important point to realize is that, for an athermal device, the effective index of refraction and its temperature dependance are the most important parameters to consider and not necessarily the individual n_i of each material. Although, individual material indices and index contrast are important for other reasons, namely, light confinement. The factors that affect the effective index of refraction are the distribution of the guided mode in the waveguide and the index contrast of the waveguide materials. If, for instance, most of a guided mode is concentrated near the core/cladding interface, n_{eq} will be closer to an average of n_f, n_s, and n_c compared with a waveguide in which the guided mode is confined mostly in the core material, and the effective index is very nearly the core's index. Where guided modes are confined in a waveguide, is a function of the particular geometry of the waveguide along with the index contrast in the waveguide. Achieving athermal operation is therefore a problem of both engineering design and materials selection.

Chapter 3

Design Considerations

One athermal design possibility, which has already been mentioned, is the pairing of materials with negative and positive thermo-optic coefficients such that the total effective index changes very little with temperature. A second possibility is to confine light in a waveguide in such a way that much of the mode is guided in a material with a very small thermo-optic coefficient, and thereby avoid having to pair two materials with potentially very different, and perhaps, incompatible mechanical properties. Both ideas have very significant materials challenges which will be discussed.

3.1 Paired Thermo-Optic Coefficients

The idea that two materials with complementary thermo-optic coefficients might be paired to minimize the effective thermo-optic coefficient of the device is, in theory, quite possible. Unfortunately, most materials are known to have positive thermo-optic coefficients, and at present, only a few polymers are known to have negative thermo-optic coefficients. If the goal were to make an athermal waveguide simply for research purposes, that goal might be very realizable. However, the goal is to create an athermal waveguide that is also compatible with current standards in CMOS processing.

CMOS processes add several important constraints to the problem of materials selection. All materials must be able to withstand the high processing temperatures

of various processing steps involved in producing IC's. Additionally, all the materials need to be robust enough to pass through the wet and dry etch processes. A final important consideration is that the semiconductor industry would prefer to use well understood materials; materials which are already being used in current CMOS processes should be given first consideration as potential materials in the athermal waveguide.

Following from the above constraints, the materials which are most often focused on as potential candidates for an athermal waveguide are silicon, silicon dioxide, silicon nitride, poly(ether imide) (PI), and poly(methyl methacrylate) (PMMA). Of these materials, silicon has the highest index of refraction and can be used for high index contrast and very good mode confinement, but its thermo-optic coefficient is also relatively high. Silicon dioxide has a very low thermo-optic coefficient, but also a very low index of refraction making it challenging to confine light in silica waveguides. The two polymers have low indices of refraction and negative thermo-optic coefficients, but each polymer's mechanical properties are very different. PI is stable up to high temperatures of 200°C while PMMA is only stable to temperatures of about 100°C. Below is a table of indices of refraction and thermo-optic coefficients for each of the above materials.

Material	Index (n)	T-O Coeff. (1/K)
Silicon	3.477	1.8×10^{-4}
Silicon Dioxide	1.444	1.1×10^{-5}
Silicon Nitride	1.974	$\sim 1.1 \times 10^{-5}$
PI	1.655	-1.2×10^{-3}
PMMA	1.6	-1.0×10^{-4}

Table 3.1: Table showing the indices of refraction and thermo-optic coefficients for several CMOS compatible materials at 1.55 μm light [1] [2].

Several material pairings are possible, for example, silicon with either polymer or silicon nitride with either polymer. Whatever the pairing, the cross-sectional dimensions of the waveguide will have to be tuned so that the guided mode takes advantage of the complementary thermo-optic coefficients and produces an athermal response to temperature. For instance, if the guided mode remains confined in the silicon, the

effective index of the waveguide will still follow the thermal response of silicon.

3.2 Guidance in Low Index Material

Guiding light in a material with a low thermo-optic coefficient is another promising way to achieve athermal operation. If, instead of using silicon as the core material, silicon dioxide is used, for instance, with a thermo-optic coefficient of 1.0 x 10^{-5} K^{-1}, the change in index may be small enough over the temperature range expected in IC's that the guided modes remain within the tolerance window for the waveguide. The problem with trying to confine modes in the silicon dioxide is that silicon dioxide has a very low index of refraction. It becomes a challenge to find a suitable cladding material that will provide a good enough index contrast to keep the mode confined in the silicon dioxide.

A few different approaches have been researched for guiding light in a low index material. All of the approaches involve taking advantage of the evanescent field which appears in all waveguides at the interface of two materials with index contrast. An early approach to this problem relied on anti-resonant reflection and total internal reflection to confine line in the low index silica (Figure 3-1). The approach involved depositing a thin layer of silicon (0.1 μm) on top of a silica substrate (2 μm), and then the core of the waveguide was a thick silica layer (4 μm) on top of the silicon. The air-silica interface confined light by total internal reflection, and at the silicon-silica interface, wavelengths which cannot resonate within the silicon, move into the top silica core and are confined [9]. Unfortunately, there are several problems with this approach; the dimensions are too large for viability in today's IC's, the confinement mechanism introduces large losses for many wavelengths, and the wavelength range over which this method functions is too narrow for WDM applications.

A second approach involves taking advantage of the discontinuity in the TE mode at high index contrast interfaces. This approach relies on Maxwell's equation for the normal electric flux density, D, at the interface of two different dielectrics:

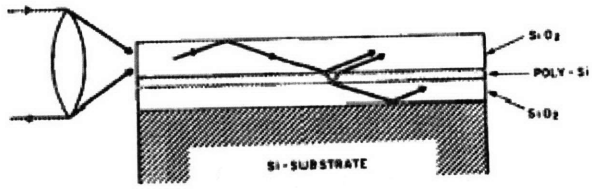

FIG. 1. Waveguide structure using antiresonant reflection on silicon wafer.

Figure 3-1: Low-index guiding by antiresonant reflection

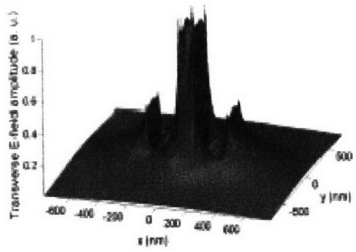

Figure 3-2: Field distribution in slot waveguide [11]

$$D = n_1^2 \varepsilon_0 E = n_2^2 \varepsilon_0 E$$

In the above expression, ε_0 is the permittivity of free space and E is the electric field [7]. On either side of an interface with materials of different indices of refraction, n_1 and n_2, the electric field becomes discontinuous with the E-field in the low index material much higher than in the high index material. The ratio of intensity of the E-field on either side of the interface is ${n_1}^2/{n_2}^2$. For a high index contrast interface, such as silicon and silica, the discontinuity produces an electric field in silica nearly 6 times higher than in silicon (see Figure 3-2). This field decays rapidly in the silica as an evanescent field [11].

To take advantage of this discontinuous increase in the TE mode at the interface of silicon and silica or any high index contrast interface, the mode has to be confined somehow. By positioning two high index contrast interfaces in very close proximity to each other, i.e. within the decay length of the electric field, the TE mode can be

confined within the low index material. Since the size of the low index slot or gap must be very small ($\langle 0.100\ \mu m$) to confine the TE mode, the waveguide inherently has a very small footprint. This approach can also guide light across a large range of wavelengths making it attractive for WDM applications.

Chapter 4

Polymer Slot Waveguide

The slot waveguide appears to be a promising approach to confining light in a low index material. This paper combines both approaches mentioned, combining guiding in a low index material with thermo-optic coefficient pairing. The purpose of combining the two methods is to realize the best athermal waveguide possible. In the polymer slot waveguide, a polymer is used as the low index material and silicon provides the high index contrast. Light is guided in the low index material according to the preceding analysis. Additionally, since most of the light is confined in the low index material and at the high index interface, the effective index of refraction for the device more closely follows the temperature dependance of the low index material than of silicon. This is desirable since the thermo-optic coefficient of the low index material is presumably negative, satisfying the criteria for athermal operation, namely $dn_{eq}/dT \leq 0$.

Polymers also offer another distinct advantage over silica as the low index material: their mode of thermal expansion. In a slot waveguide, the width of the slot makes a substantial difference in the effective index of the slot waveguide and in the intensity of the guided mode. As silicon dioxide expands, it may cause strain on the high index silicon, and may widen the slot as it expands thermally. On the other hand, as polymers expand, they flow in the direction in which such flow is unrestricted, in this case, out of the slot. Instead of placing strain on the silicon and expanding the slot, the slot width remains constant.

Polymers are also easy and inexpensive to deposit, even if strictly uniform films are hard to realize. For this application, the uniformity of the film is not critical since the light is being guided inside the vertical slot and is not dependant on the film thickness or roughness at the polymer-air interface. Losses, however, are dependant on the surface roughness of the silicon at the polymer-silicon interface. Surface roughness is an ongoing problem for silicon and other high index contrast waveguides and is the subject of much academic and industrial study; however, the subject of surface roughness is beyond the scope of this paper.

The polymer slot waveguide consists of a silica substrate on which is deposited two silicon rims. Each rim is meant to be approximately 0.150 - 0.300 μm in width and about 0.200- 0.400 μm in height. The slot may not exceed the decay length of the evanescent field given by:

$$E(r) \propto e^{(-\gamma r)}$$

where γ is the attenuation coefficient and describes the exponential decay of the evanescent field a distance, r, away from the center of the core, in this case silicon. For slot waveguides including the polymers PI and PMMA, the slot width may not exceed 0.070 μm (see Appendix A). The slot is filled by the polymer which is spin coated on top of the silicon and silica substrate.

The polymer slot waveguide is a compact solution to confining light in low index materials. By performing simulations of the polymer slot waveguide, taking into account the thermo-optic coefficients of the various materials in the waveguide, this research hopes to provide a potential solution for athermal, CMOS integration, of optical waveguides.

Chapter 5

Experimental Design

5.1 Simulation

Computer simulations of varying waveguide designs were used to gain an understanding for how different materials and cross-sections affect the effective index of refraction in the device. Simulations can be very powerful modeling tools, but have their limitations. In this case, APSS version 2.3 was used to simulate three different waveguide cross-sections. APSS allows the user to specify the dimensions of a 2-D cross-section of any waveguide, including the index of refraction of each material in the core, cladding, substrate, layers, etc. APSS then uses a mesh to calculate by finite element analysis the confinement of the guided modes within the waveguide and a host of other relevant measures including effective index of refraction. The software package includes a function that allows for the adjustment of the mesh size.

Because the software must operate on a computer with fixed processing capacity, there are limitations to the minimum mesh size and the number of meshes. The implications of a limit on mesh size are a limit on the precision of simulation results. When cross-sectional dimensions are changed but the change does not affect how the waveguide is split by the mesh, the simulation will show no change in effective index or confinement. This occurs when dimensional changes are on the order of the smallest mesh. In order to squeeze the most processing power from the computers, an irregular mesh size is used to highlight the interfaces of different materials, and in the

regions of secondary interest, the mesh is left with fairly sparse coverage. The average mesh concentration for the slot waveguide simulation was about 150/μm within the low index gap.

5.1.1 Channel Waveguide

The first simulation performed was of a simple rectangular channel waveguide. A channel waveguide consists of a core surrounded on all sides by the lower index cladding material. Light is confined in the high index material used as a core. For this simulation, the core was comprised of silicon and the cladding material used was the low index material, silicon dioxide.

The dimensions of the calculation window were 3 μm by 5 μm. The cross-sectional dimensions of the channel were varied from 0.100 μm to 0.500 μm in height and from 0.250 μm to 1.00 μm in width. APSS allows for one variable to be adjusted at a time holding all other things constant. For all of the simulations the wavelength was held constant and either the height or the width of the core was varied. The wavelength of light was held constant in the infrared range at 1.55 μm. At this wavelength the index of refraction of silicon is 3.477 and the index of refraction for silicon dioxide is 1.444 [2].

5.1.2 Modified Rim Waveguide

The second simulation performed was of a modified rim waveguide. The rim waveguide structure is similar to a channel waveguide in that it consists of a channel core. The difference between a rim waveguide and a channel waveguide is that two different materials may comprise the cladding on top and beneath the core. In this case, the silicon channel or rim is deposited on a silicon dioxide substrate and then a polymer is deposited on top of both. For the modified rim waveguide, the silicon rim may be partially "buried" in the silicon dioxide substrate (see Figure 5-1).

For this simulation, the calculation window was 5 μm by 10 μm. The cross-sectional height of the rim was varied from 0.200 μm to 2.00 μm while the cross-

sectional width of the rim was varied from 0.500 μm to 5 μm. The degree to which the silicon rim was "buried" in the oxide was also varied from 10% to 100% coverage of the silicon rim side walls. The index of refraction values used for each material were 3.477 for silicon, 1.444 for silicon dioxide, and 1.655 for the polymer [2]. The polymer modeled was a kind of poly(ether imide).

5.1.3 Slot Waveguide

The final simulation performed was of a slot waveguide. The slot waveguide consists of two rims deposited very close together on a substrate so that a narrow gap or slot exists between them; a cladding material is then deposited on top and around the rims, filling the slot and covering the rims. The rims are silicon deposited on a silicon dioxide substrate and covered by a polymer cladding (see Figure 5-1).

For this simulation, the calculation window was 3 μm by 6 μm. The cross-sectional height of each rim was varied from 0.100 μm to 0.500 μm and their width was varied from 0.100 μm to 0.400 μm. The slot width was varied from 0.010 μm to 0.100 μm. The model used an index of refraction of 3.477 for silicon, 1.444 for silicon dioxide, and 1.655 or 1.6 for the polymer [2]. The two types of polymers modeled were poly-(ether imide) (PI) and poly-(methyl methacrylate) (PMMA).

5.2 Thermo-Optic Coefficient

The thermo-optic coefficient of the two polymers was needed in order to accurately model the proposed athermal device. The thermo-optic coefficient of the two polymers, PI and PMMA, was measured using an ellipsometer and a heating stage. The ellipsometer requires the polymer film thickness as an input in order to calculate an index of refraction for the film. The polymer film thickness was measured using a profilometer.

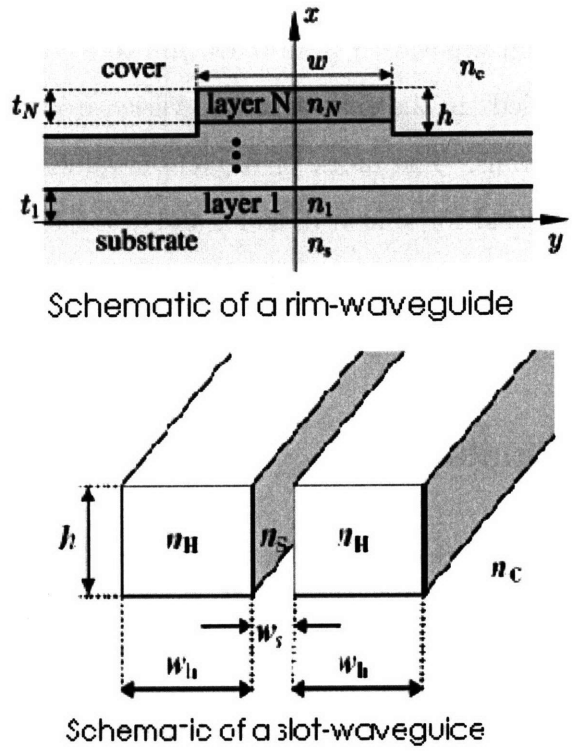

Figure 5-1: Schematic diagrams of a rim [3] and slot [7] waveguide

5.2.1 Polymer Spin Coating

Spin coating of each polymer was performed using a Specialty Coating Systems, Spin Coater 6700 Series. The PI used was Pro-Lift 100-24. Before spin coating the PI, the silicon wafer was pre-baked at 100°C to evaporate any moisture remaining on the silicon surface. The PI was spin coated by setting the spin coater to spin at 2500 rpm for 90 s. Spinning at this rate produces a uniform thin film of PI with a thickness of approximately 2 μm. The polymer coated wafer was then immediately placed on a hot plate heated to 150°C to soft-bake the polymer for 90 s. After the soft bake, the hot plate's temperature was raised to 250°C and the wafer was baked for another 90 s.

The PMMA was deposited in an analogous fashion. The PMMA used was MicroChem 950PMMA A resist. First, the silicon was pre-baked at 100°C to remove any moisture on the silicon surface. The PMMA was then spin coated onto the silicon wafer by setting the spin coater to spin at 1000 rpm for 45 s. Spinning at this rate

produces a uniform thin film of PMMA with a thickness of approximately 1 μm. The polymer coated wafer was then baked at 180°C for 90 s.

5.2.2 Profilometry

In order to accurately and precisely measure the average polymer film thicknesses, a Tencor P-10 Surface Profilometer was used. Each wafer was cleaved into small sections of about 1 cm^2 using a diamond cleaver. Using the edge of a razor, the polymer film of at least one section was scratched off in a line such that the silicon wafer was exposed in the scratch. This scratch produces a step increase in height from the wafer level to the polymer film level allowing the profilometer to make a more accurate assessment of the film thickness. Several different scratches were made on a single section in order to ascertain that the film was indeed deposited in a uniform fashion.

Each scratched wafer section was then placed in the profilometer to measure the film thickness. Each scratch was passed over perpendicular to the direction of the scratch 3 times, and an average was taken of the film thickness.

5.2.3 Ellipsometry

The profilometry results for the thickness of the polymer thin films were used in conjunction with the Gaertner Scientific 3-Wavelength Variable Angle Ellipsometer in order to find the index of refraction of each polymer, PI and PMMA. A measurement of the thermo-optic coefficients of each polymer was achieved by using a Linkum Scientific FTIR 600 Freezing/Hotstage to control the temperature of the wafer and simultaneously measure the index of refraction in 5°C steps. The incident wavelength of light was 633 nm.

5.3 Athermal Slot Waveguide Simulation

The simulated slot waveguide did not have any adjustments of the index of refraction for temperature, therefore an estimation of its response to temperature was not yet made. In order to make an estimation of the device thermo-optic coefficient, the thermo-optic coefficients of each material in the device need to be input into the model. Since the thermo-optic coefficient can be assumed to be constant even for very different wavelengths of light, the thermo-optic coefficients measured at 633 nm can still be used to estimate the optical response to temperature even at incident wavelengths of 1.55 μm.

The measured thermo-optic coefficients for the polymers along with widely accepted thermo-optic coefficient values for the silicon and silicon dioxide, were used to create a table of indices of refraction corresponding to particular temperatures. In order to use APSS to find the thermo-optic coefficient of the device, each index of refraction corresponding to the temperature of interest was input into the model. With the properties of each material at the desired temperature in place, the cross-sectional dimensions of the waveguide could then be varied, simultaneously, to create a design space in which a specified slot width, for example, corresponds to a specific effective index of refraction and a specific device thermo-optic coefficient. A simulation of the slot waveguide design was conducted separately for both types of polymer, PI and PMMA.

Chapter 6

Results

The results of this research are described below. The results reported are limited to the results which are particularly relevant to the design of an athermal waveguide. They do not include the results from the first simulations as those were primarily used to gain an intuition for appropriate mesh sizes and other simulation parameters. The results reported include a discussion of the measurement of the thermo-optic coefficient of the two different polymers and of the polymer slot waveguide simulations.

6.1 Polymer Film Optical Properties

The spin coated polymers were deposited fairly uniform across the silicon wafers. The PI was significantly more viscous, and did not form a film as uniformly as the PMMA. The profilometer gave a mean film thickness for PI of 1.727 ± 0.005 μm. The mean film thickness for PMMA was measured as 0.907 ± 0.005 μm. The lack of uniformity is not reflected in the film thickness measurement because wafer sections were selected for their relative uniformity.

These film thicknesses were used to assist the ellipsometer in calculating the index of refraction for each polymer. The ellipsometer radiates 633 nm light; therefore, the index of refraction taken from the ellipsometer measurements does not reflect the appropriate index of each polymer at 1.55 μm, the wavelength used for the simulations. The ellipsometer is used to simply calculate the thermo-optic coefficient, which is

assumed to be constant or nearly constant across all wavelengths.

To measure the thermo-optic coefficient, a heat stage was used to control the temperature from below the wafer. The wafer was mounted onto a glass slide which was then placed onto the silver heating stage. With multiple layers between the heating stage surface and the polymer, precise control of the temperature of the polymer is difficult. The radiative losses were minimized by using only a small wafer section, 1 cm^2. However, there are still some heat losses as the distance from the heating stage increases. It is important to understand that this systematic error exists. Additionally, as the polymer was heated, its thermal expansion was not considered, and the film thickness was not adjusted. Figure $6-1$ shows the thermo-optic coefficients as measured using the ellipsometer and heating stage.

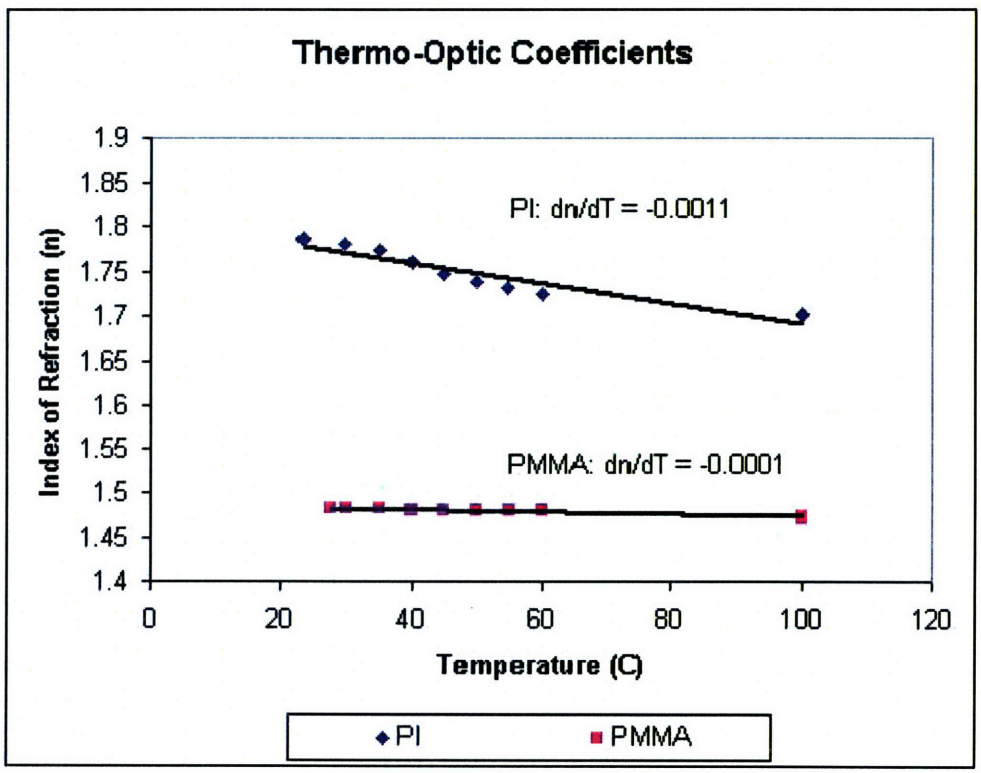

Figure 6-1: T-O Coefficient for PI and PMMA

Although the results are not perfect from an experimental point of view, they are in agreement with values for the thermo-optic coefficient of PI and PMMA found in literature. These values are sufficient for the simulation of the slot waveguide that will

incorporate thermo-optic coefficients. The goal is simply to understand the impact of a material with a negative thermo-optic coefficient on the effective thermo-optic coefficient of the entire device.

6.2 Simulation

The initial goal is to create a design space for tuning the index of refraction of the slot waveguide simply by changing the cross-sectional geometry. The standard slot waveguide and its variable dimensions are shown in Figure $6-2$.

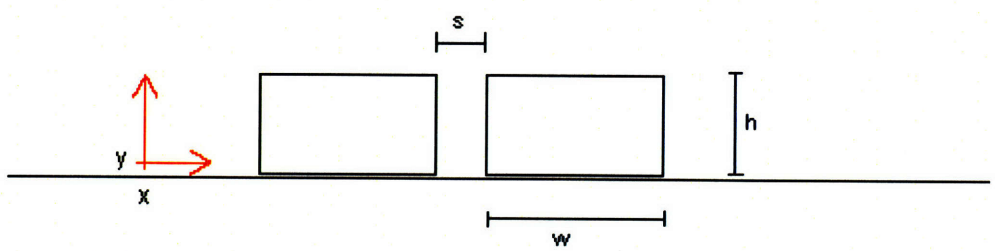

Figure 6-2: Cross-section of a slot waveguide

The index of refraction can be tuned by changing the various dimensions shown in Figure $6-2$. Simulations of the slot waveguide using a PI cladding, silica substrate, and silicon rims yielded the relationship between effective index and the two geometric parameters, width and height shown in Figures $6-3$ and $6-4$.

In both cases, increasing the width or height of the high index material increases the effective index of the waveguide. This is an expected result since more high index

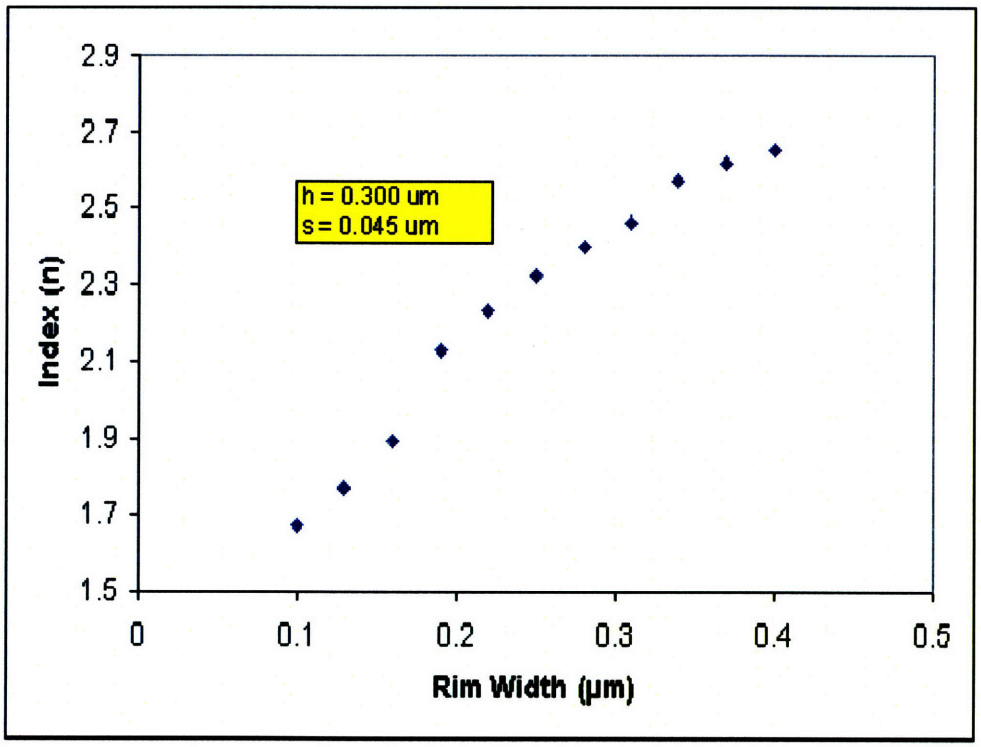

Figure 6-3: Effective index tuning by changing rim width, w

area allows a greater percentage of the guided mode to be confined within the silicon. In the rim width regime 0.100 - 0.400 μm, the effective index increases by about 3.4 x 10^{-3} nm^{-1}. However, the relationship between $n_(eq)$ and $w$is not linear. Similarly, within the rim height regime analyzed (0.100 - 0.500 μm), the effective index increases by approximately 1.3 x 10^{-3} nm^{-1}. The effect of increasing the height has a less overall effect on the effective index since the most important mode is the guided TE mode; the TE mode in the x-direction is evanescent.

The final variable that can be adjusted to change the effective index is the slot width (see Figure $6-5$). Unfortunately, the mesh size in the simulation package could not be adjusted to a suitably fine degree due to the risk of crashing the computer; the mesh size imposed a limit on how finely the software could simulate a change in effective index with changing slot size. In figure $6-5$, there is a clear step in the effective index which corresponds to the point where the change in slot width finally cleared a new mesh, and the software was able to calculate a change in effective index.

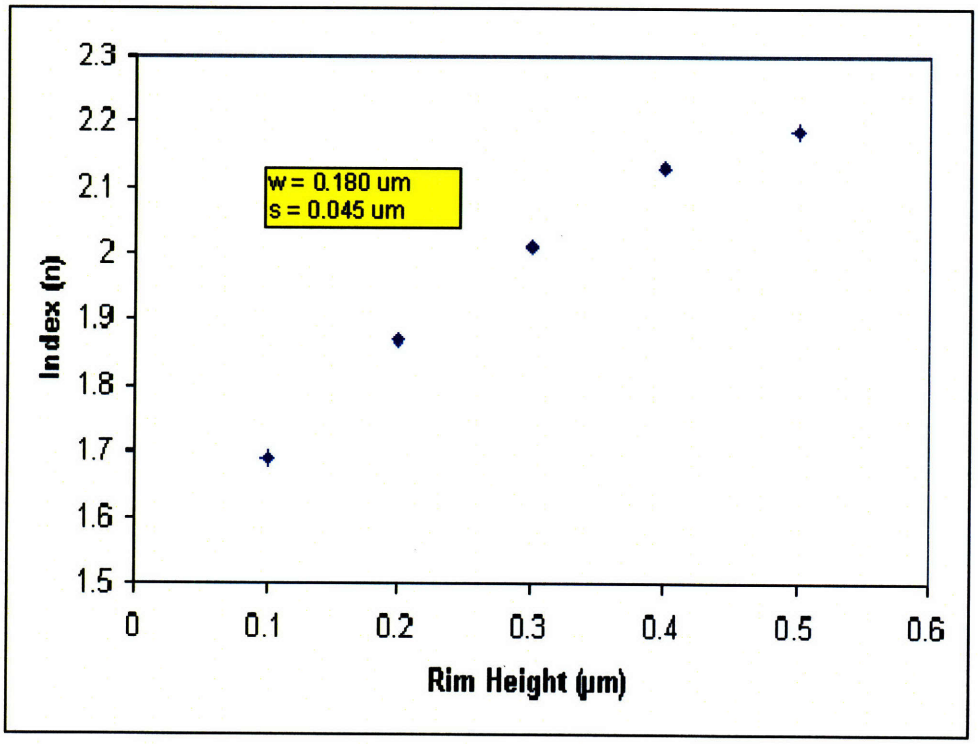

Figure 6-4: Effective index tuning by changing rim height, h

Perhaps counterintuitively, increases in the low index slot material area also have the effect of increasing the effective index of the waveguide. Recall that the method by which light is confined in the low index material is by the coupling of two evanescent fields; as the high index contrast interfaces move farther apart and the gap width closer to the decay length of the evanescent field, the smaller the coupled intensity will be compared to the light intensity guided within the high index material, near the high index contrast interface. The effect of shifting the distribution of the guided mode from the low index material to the high index material causes the effective index of refraction for the entire waveguide to increase.

Ideally, the index of refraction would be tuned simply by adjusting the slot width. In CMOS processing, the slot width would be the easiest parameter to change. Therefore, the final simulation to test the thermo-optic coefficient of the device holds the rim height and width constant at 0.300 μm and 0.180 μm, respectively while varying the slot width and operating temperature. The temperature is artificially adjusted by

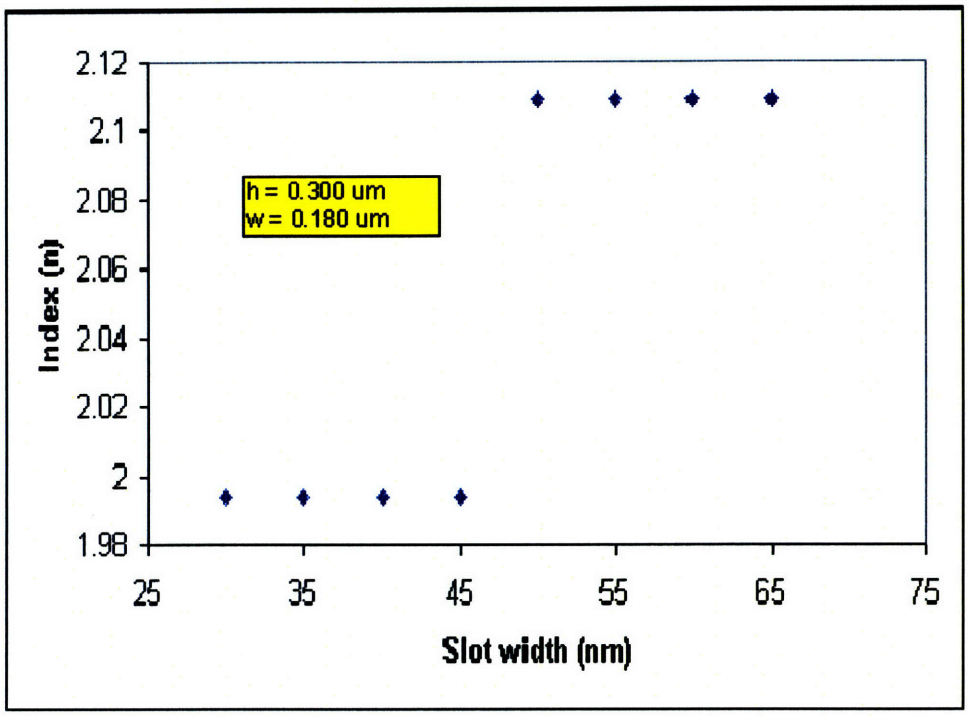

Figure 6-5: Effective index tuning by changing slot width, s

incorporating the thermo-optic coefficient into the refractive indices of each material.

For the PI slot waveguide, the magnitude of the thermo-optic coefficient of the device with the larger slot size is smaller than the thermo-optic coefficient for the device with the smaller slot size, -8.0 x 10^{-4} at 0.065 μm compared with -9.0 x 10^{-4} at 0.045 μm (see Figure $6-6$). This result can be explained by the magnitudes of the relative thermo-optic coefficients of silicon and PI. The magnitude of silicon's thermo-optic coefficient is about 10x smaller than the thermo-optic coefficient measured for PI. In the device, this difference means that for small slot widths, when the mode is almost entirely confined in the slot, the thermo-optic effect of PI dominates. However, as the slot size is increased, less light is confined in the slot and more light closer to the silicon interface, and the magnitude of the thermo-optic coefficient decreases slightly.

In the PMMA device, the effect is the opposite. Since the thermo-optic coefficient of silicon is larger in magnitude than the thermo-optic coefficient of PMMA, at narrower slot widths, with most of the light concentrated in the low thermo-optic

domain, the thermo-optic coefficient of the device decreases. For the PMMA slot, the effective thermo-optic coefficient is always positive at the slot widths simulated due to this magnitude difference in thermo-optic coefficients between silicon and PMMA. For a slot width of 0.065 μm the effective thermo-optic coefficient is 4.0 x 10^{-6} K^{-1} and 3.0 x 10^{-5} K−1 for a slot width of 0.045 μm (see Figure 6 – 7).

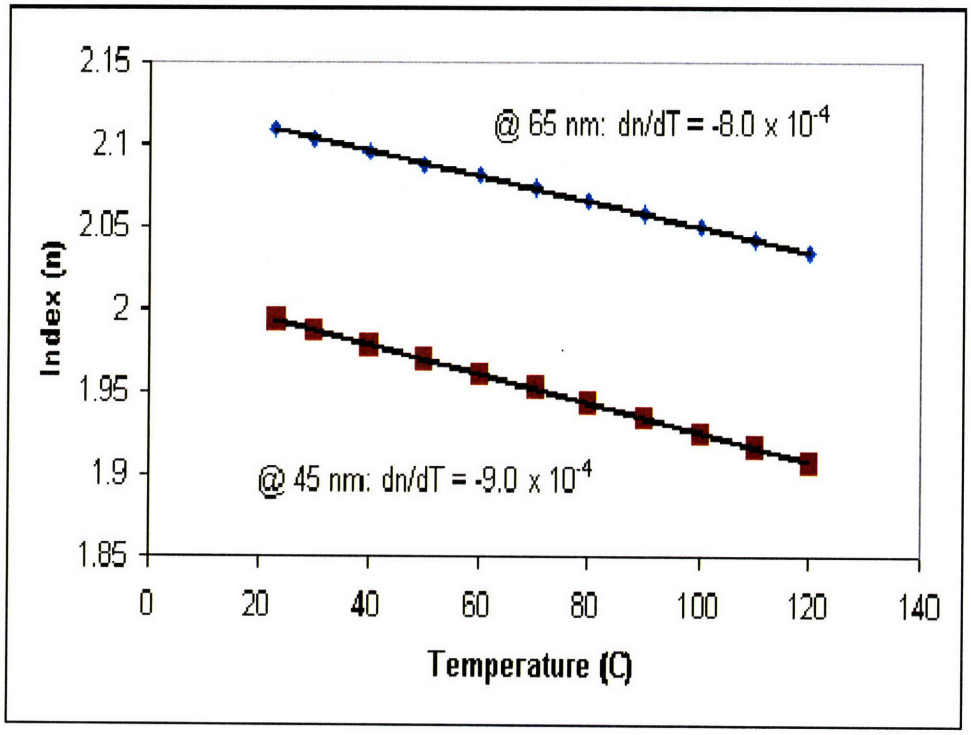

Figure 6-6: Thermo-optic coefficient of PI slot waveguide

6.3 Conclusion

The polymer slot waveguide appears to be a viable solution for CMOS compatibility and athermal mode confinement. The following design rule holds for athermal design:

$$\Gamma = \frac{P_f}{(P_c + P_f + P_s)} = \frac{\frac{dn_c}{dT}}{\left(\frac{dn_s}{dT} + \frac{dn_c}{dT} + \frac{dn_f}{dT}\right)}$$

where Γ is the confinement factor for the waveguide and the subscripts denote the parts of the waveguide. The above expression holds only for pairing complemen-

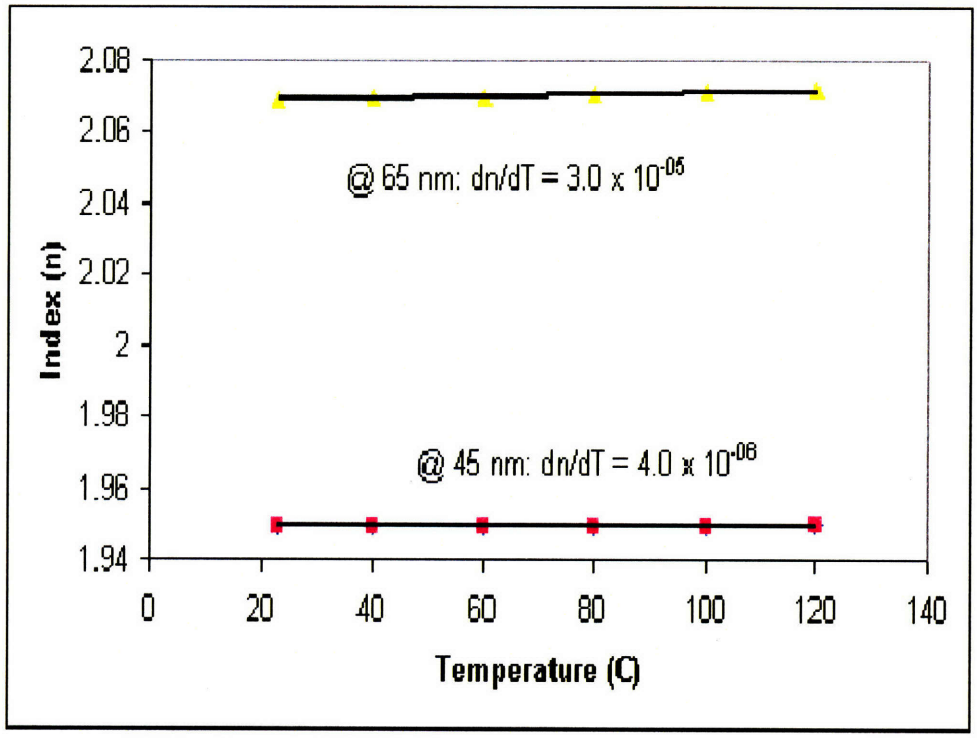

Figure 6-7: Thermo-optic coefficient of PMMA slot waveguide

tary thermo-optic coefficients, and n_i above are the magnitudes of each thermo-optic coefficient. For example, in a waveguide in which 25% confinement is in the high thermo-optic material, the cladding material need have a thermo-optic coefficient of only 33% that of the core. Following from above, a PI slot waveguide with larger slot width (⟩ 65nm) will yield a smaller effective thermo-optic coefficient than has been simulated, but some compromise will have to be made in terms of mode confinement and guided mode intensity. The current, simulated confinement factor is 19.4% in PI. A better athermal design incorporating PI would be to design a simple silicon rim waveguide with a PI cover so that a greater percentage of the mode is confined in silicon ($\sim$ 90%). A PMMA slot waveguide seems especially viable in terms of providing athermal behavior, especially at small slot widths; however, questions remain about the thermal durability of the PMMA in a high temperature environment. The simulations show promise that an athermal polymer slot waveguide could be realized. However, a real athermal polymer slot waveguide has yet to be fabricated, and

testing of the real mode confinement will need to be conducted to ascertain the simulated results. Polymer film thickness and silicon sidewall roughness will be significant concerns in the future production of polymer slot waveguides.

Appendix A

Figures

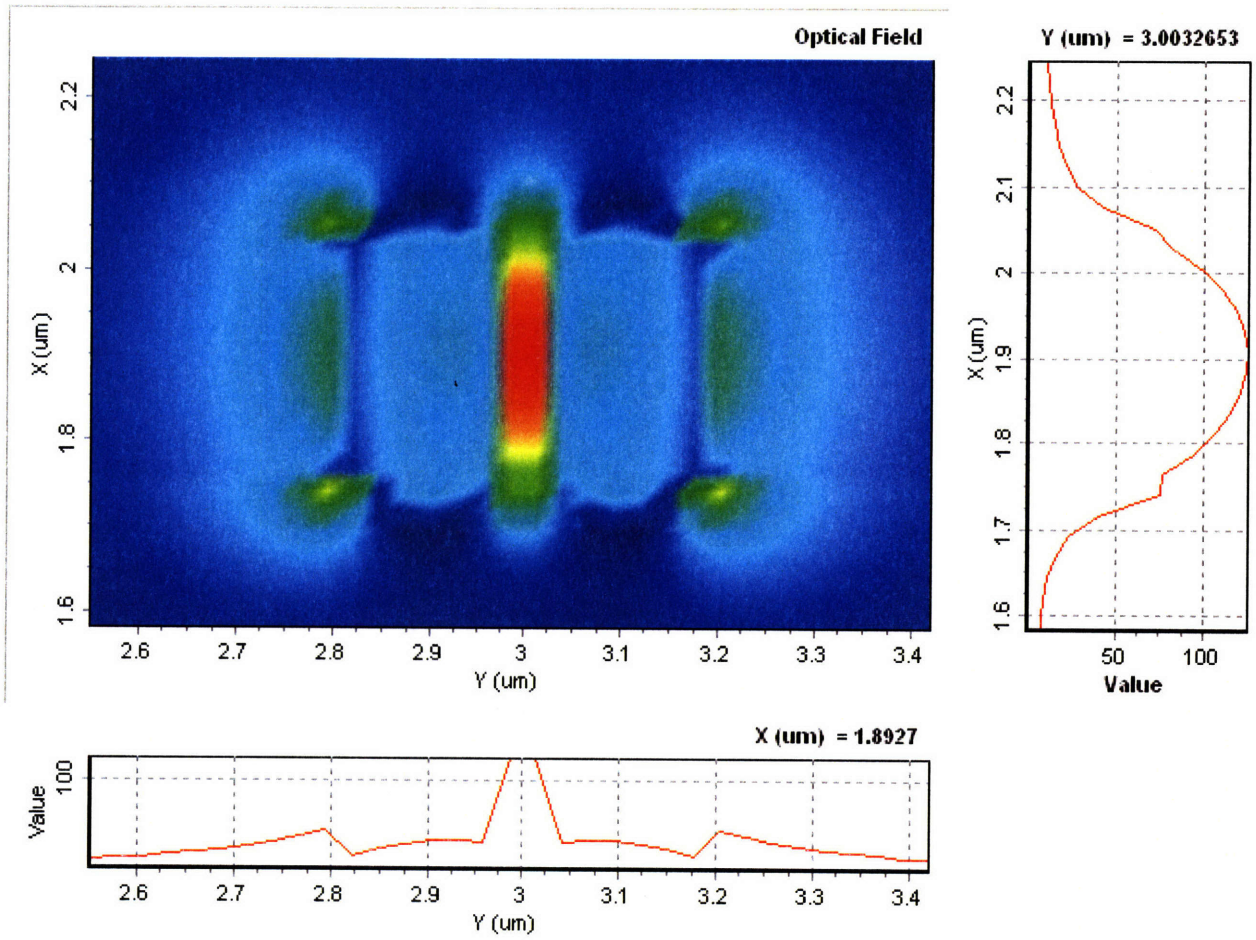

Figure A-1: Mode intensity and confinement in a PI slot waveguide, slot width = 45 nm

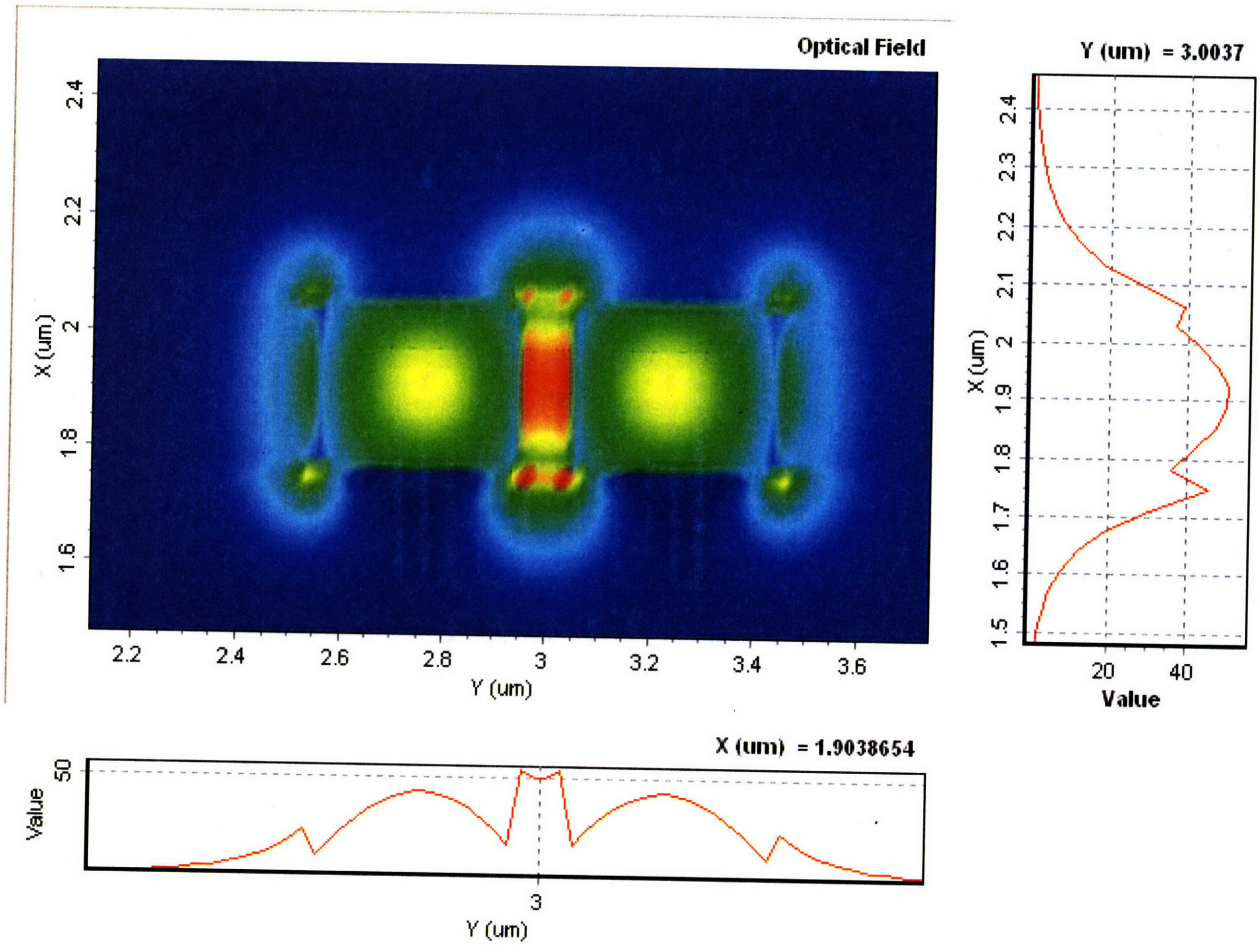

Figure A-2: Mode intensity and confinement in a PI slot waveguide, slot width = 80 nm

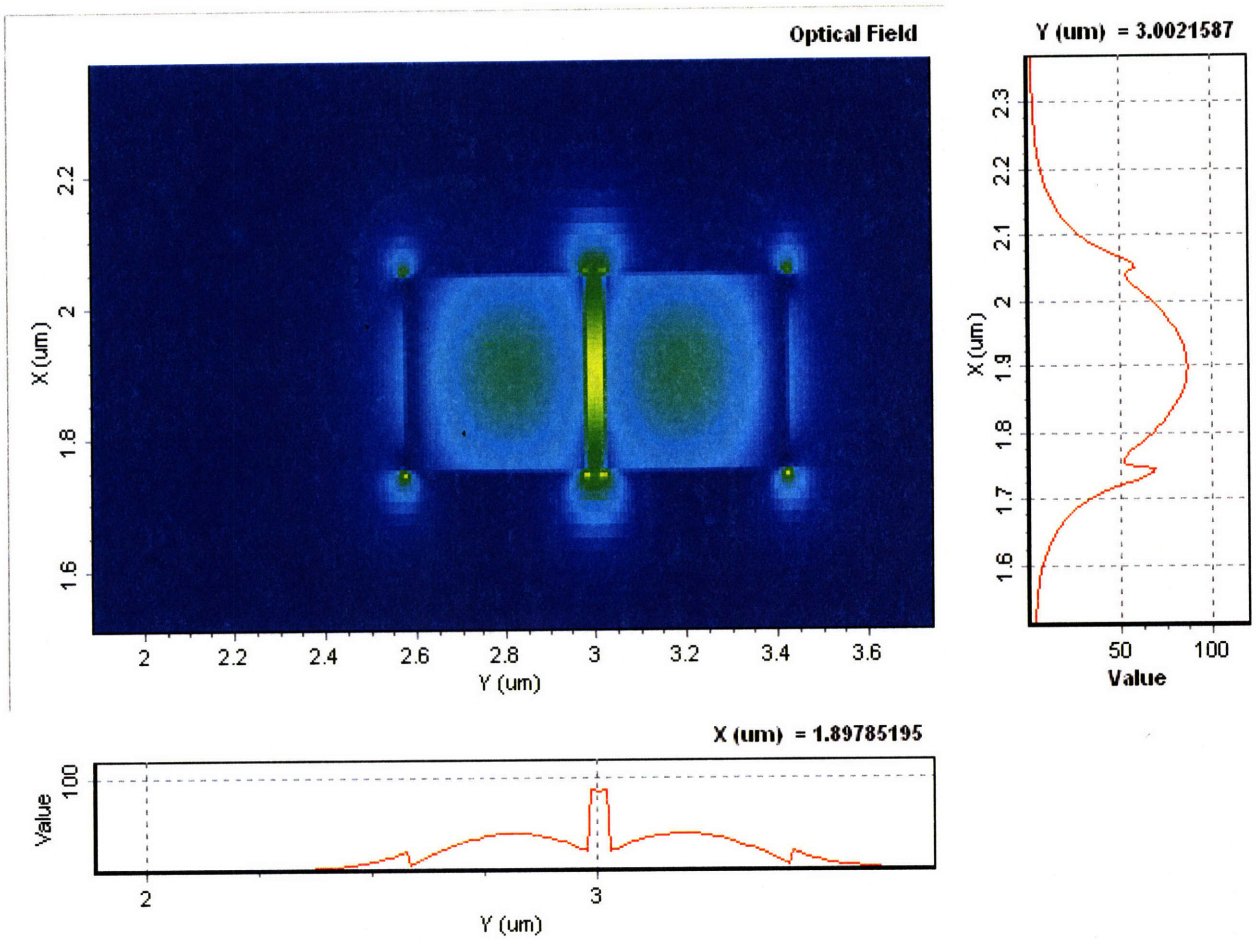

Figure A-3: Mode intensity and confinement in a PI slot waveguide with increase rim width, rim width = 400 nm

Bibliography

[1] Luoay Eldada. Polymer integrated optics: promise vs. practicality. Technical report, Dupont Photonics Technologies, Wilmington, MA, 2004.

[2] Yoel Fink. Database of optical constants. website. accessed Mar 2007.

[3] Manfred Hammer. Guided light propagation in planar dielectric films. website. accessed May 21, 2007.

[4] Gilbert Held. *Understanding Data Communications*, volume 1, chapter 7. New Rider Publishing, Norwell, Massachusetts, 6 edition, 1999.

[5] Keigo Iizuka. *Elements of Photonics*, volume 2, chapter 9-10. Wiley-Interscience, New York, NY, 2002.

[6] Clifford Pollock; Michal Lipson. *Integrated Photonics*, volume 1, chapter 3, pages 43–71. Kluwer Academic Publishers, Norwell, Massachusetts, 2003.

[7] Vilson R. Almeida; Qiantan Xu; Roberto R. Panepucci; Carlos A. Barrios; Michal Lipson. Light guiding in low index materials using high-index-contrast waveguides. Number 797 in Materials Research Society Symposium Proceedings, pages 1–6, Boston, MA, October 2004. MRS, Academic Press.

[8] Donald N. Merino. Assessing technological forecasts for the fiber-optic communications market. *IEEE Transactions on Engineering Management*, 37(1), February 1990.

[9] M. A. Duguey; Y. Kokubun; T. L. Koch; Loren Pfeiffer. Antiresonant reflecting optical waveguides in "sio_2-si" multilayer structures. *IEEE Photonics Technology Letters*, 49(17), July 1986.

[10] Yasuo Kokubun; Norihide Funato; Masanori Takizawa. Athermal waveguides for temperature-independent lightwave devices. *IEEE Photonics Technology Letters*, 5(11):1297–1300, November 1993.

[11] Qianfan Xu. Experimental demonstration of guiding and confining light in nanometer-size low-refractive-index material. *Optics Letters*, 29(14):1626–1628, July 2004.